Available online at www.sciencedirect.com

jmr&t
Journal of Materials Research and Technology

journal homepage: www.elsevier.com/locate/jmrt

Original Article

Effect of sugar palm fibers on the properties of blended wheat starch/polyvinyl alcohol (PVA) -based biocomposite films

Abdulrahman A.B.A. Mohammed [a], *Zaimah Hasan* [a,**], *Abdoulhdi A. Borhana Omran* [b,c,*], *Abdulhafid M. Elfaghi* [d], *Yasir Hassan Ali* [e], *Norie A.A. Akeel* [b], *R.A. Ilyas* [f,g,h], *S.M. Sapuan* [h]

[a] *Department of Mechanical Engineering, College of Engineering, Universiti Tenaga Nasional, Jalan Ikram-Uniten, Kajang 43000, Selangor, Malaysia*
[b] *Department of Mechanical and Mechatronic Engineering, Faculty of Engineering, Sohar University, Sohar, P C-311, Oman*
[c] *Department of Mechanical Engineering, College of Engineering Science & Technology, Sebha University, Sabha 00218, Libya*
[d] *Faculty of Mechanical and Manufacturing Engineering, Universiti Tun Hussein Onn Malaysia, Malaysia*
[e] *Department of Power Mechanics Techniques Engineering, Technical College Mosul, Northern Technical University Mosul, Iraq*
[f] *School of Chemical and Energy Engineering, Faculty of Engineering, Universiti Teknologi Malaysia, Johor Bahru 81310, Johor, Malaysia*
[g] *Centre for Advanced Composite Materials (CACM), Universiti Teknologi Malaysia, Johor Bahru 81310, Johor, Malaysia*
[h] *Institute of Tropical Forestry and Forest Products (INTROP), Universiti Putra Malaysia, Serdang 43400, Selangor, Malaysia*

ARTICLE INFO

Article history:
Received 16 October 2022
Accepted 5 February 2023
Available online 9 February 2023

Keywords:
Wheat starch
Biocomposite
Polyvinyl alcohol
Fructose
Sugar palm fiber

ABSTRACT

Sugar palm fiber has been added to reinforce starch, polyvinyl alcohol (PVA) based film. The effect of reinforcement on different properties has been studied. It has been found that reinforcing plasticized starch/PVA matrix with palm fibers has considerably enhanced physical properties, the density of the polymer declined to 1.21 g/cm^3 with untreated fibers and to 1.32 g/cm^3 with treated fibers, which created a lighter weight bioplastic, and a reduction occurred in water absorption (for example 3% of treated fiber showed 143% absorbed water after 30 min immersing in water) and water solubility. When compared to the films without fibers filler, films reinforced with fibers demonstrated a c3onsiderable improvement in the crystal profile; at 9% fiber load, it improved over double. Additionally, it has been noted that thermal stability has increased. The existence of treated and untreated fibers in the hybrid matrix revealed 23.3% and 24.6% mass residues at 495 °C, respectively. However, this enhancement did not coincide with a rise in mechanical properties, Whilst,

* Corresponding author.
** Corresponding author.
E-mail addresses: zaimah@uniten.edu.my (Z. Hasan), aomran@su.edu.om (A.A. Borhana Omran).
https://doi.org/10.1016/j.jmrt.2023.02.027

improvements in tensile strength and modulus occurred at 9% of treated fiber load, showing 12 MPa and 245 MPa, respectively. The highest elongation was 66.3% at 3% of treated fiber films. Meanwhile, films reinforced with treated sugar palm fibers showed higher mechanical properties than films with untreated sugar palm fibers. Scanning Electronic Microscope images exhibited higher interfacial interaction at 9% for both treated and untreated sugar palm fibers.

1. Introduction

Biocomposite materials represent a good solution to replace non-degradable plastic [1]. The development of environmentally friendly bioplastic materials, which are biodegradable, inexpensive to produce, lightweight, renewable, chemically inert and simpler to work with than most synthetic plastic materials, has shown to be the most appropriate solution [2]. Particularly for the food packaging industry, the search for suitable protective packaging made from renewable sources is increasingly important [3]. Bioplastic-based starch has some flaws such as brittleness. Plasticizers such as fructose are used to improve the flexibility [4] while blending the starch with additives synthesis polymer such as polyvinyl alcohol (PVA) [5] is a good method to improve the mechanical properties in general. Reinforcing bio-matrix with natural fibers has a considerable favorable effect [6].

Starch is a carbohydrate that accounts for 60–75% of the weight of wheat grains [7]. Because of their high decomposition rate and ability to serve as a matrix with various types of fillers, starch is an excellent choice for making biopolymers films. Starch also has additional advantages such as availability, low cost, and the capacity to enhance its properties by additives when it is used in bioplastic production. Despite various advantages of film-based starch, the production of the starch film is still limited due to the weak mechanical qualities, film's brittleness, and handling associated problems. The starch-based polymer is mostly made up of linear amylose and highly branched amylopectin. In wheat starch, amylose accounts for 20–30% of total starch, while amylopectin accounts for the rest [8]. Both PVA and starch were multi-hydroxyl polymers with hydrophilic characteristics and changeable qualities depending on the humidity of the environment [9]. PVA repeating units include a hydroxyl group, which enables it to cross-link with other polymers like amylose and cellulose chains via linked hydrogen bonds [10].

Because all parts of the sugar palm tree, including palm sap, trunk, fruits, and leaves, can be used, it is known as a multi-purpose tree. Fiber is another product of the sugar palm tree. Sugar palm fibers can be found in several portions of the tree that can be classified into; black sugar palm fibers (ijuk), sugar palm bunches (SPB), sugar palm fronds (SPF), and sugar palm trunks (SPT). Previous research has found that sugar palm fibers have good tensile and physical characteristics and can be used as reinforcing agents in composite materials. Fiber can be collected from various portions of the plant and used as a reinforcing filler in natural and synthetic matrixes. Surface treatment is a technique for cleaning, modifying, and improving the fiber surface to reduce surface tension and improve the interaction of the fiber filler with the starch film matrix or synthesis matrix [11,12].

This work aims to study the effect of treated and untreated sugar palm fibers loading on biodegradable matrix. Even while the inclusion of PVA considerably enhanced the mechanical properties in our earlier research. It had some negative effects on the material's physical and thermal characteristics. In order to address and reduce these limitations, we added fibers in this study.

2. Materials and methods

2.1. Materials

Wheat starch and palm fiber have been bought from a local supplier in Kajang, Selangor, Malaysia. The wheat starch contains 83.5% carbohydrate, 0.7% protein, and 0.2% fat according to the producer company Bestari Sdn. Bhd [13]. The amylose and amylopectin percentages were measured using spectrophotometer device. Amylose and amylopectin contents were 21.91% and 78.09%, respectively. 84.5% of distributed starch particles had sizes less than 212 μm, while 100% of fiber particles were less than 212 μm. The water content of wheat starch was 0.895% and the density was 1.6 g/cm^3. Fructose was supplied by Evergreen Engineering & Resources Sdn. Bhd., Malaysia. The degree of hydrolysis of PVA is 98%–99.8%. The percentages of cellulose, hemicelluloses, and lignin were then calculated using Van Soest analysis described by the equations below [14]:

$$\text{Cellulose (\%)} = \text{ADF} - \text{ADL} \quad (1)$$

$$\text{Hemicellulose (\%)} = \text{NDF} - \text{ADF} \quad (2)$$

$$\text{Lignin (\%)} = \text{ADL} \quad (3)$$

where: ADF: Acid Detergent Fiber, ADL: Acid Detergent Lignin, and NDF: Neutral Detergent Fiber.

It has been founded that the untreated sugar palm fiber consisted of; cellulose (45.7%), hemicellulose (4.1%), lignin (33.11%) and other components (17.09%), while the treated sugar palm fiber consisted of; cellulose (82.1%), hemicellulose (0.93%), lignin (5.59%) and other components (11.38%).

2.2. Sugar palm fiber treatment

Chemical treatment has been applied to increase the amount of cellulose percentage by removing waxes, phenolics, pigments, oils, hemicelluloses, lignins, and ashes as appears in the graphical abstract. This process has been done by following the strategy below, which has been described by Coelho et al. [15].

i) Treatment with ethanol solution (1:15 m $_{\text{sugar palm fiber}}$: v $_{\text{solution}}$) at 75 °C for 3 h to remove wax, phenolics, pigments, and oils.
ii) Treatment with 2% H_2SO_4 solution (1:20 m $_{\text{sugar palm fiber}}$: v $_{\text{solution}}$) at 90 °C for 5 h to hydrolyze polysaccharides and acid-soluble polyphenols.
iii) Treatment with 5% NaOH solution (1:20 m $_{\text{sugar palm fiber}}$: v $_{\text{solution}}$) at 90 °C for 5 h to dissolve the remaining hemicelluloses, lignins, and other polysaccharides,
iv) Bleaching (1:20 m $_{\text{sugar palm fiber}}$: v $_{\text{solution}}$) with 5% H_2O_2 solution at 50 °C for 8 h for two consecutive stages.

2.3. Film preparation

5 g of isolated wheat starch was dissolved in 100 ml of distilled water and blended with 25% PVA of starch dry weight. The treated and untreated sugar palm fibers were added based on the weight of the whole blend, as shown in Table 1, the mixture was heated in a water bath where the water temperature was 85 °C with constant stirring for 20 min, after ensuring that the starch particles have been mixed and it takes a slurry shape, the plasticizer (35% w/w fructose of starch dry weight) was added to the slurry and kept stirring constantly for another 20 min. After that, the slurry was treated with an ultrasonic device to remove the bubbles and improve the adhesion between particles. 15 g of the treated slurry was cast at room temperature (RT) in Petri dishes (90 mm diameter). Then the films were placed in a dry oven for 20 h at 45 °C.

2.4. Physical properties

2.4.1. Film thickness

The film thicknesses were determined according to the method indicated by Lu et al. [16], the thickness was measured by a micrometer. The average of five different specimens was taken to represent the thickness.

2.4.2. Film density

The square dimension (2 × 2 cm^2) of films was taken to measure the density. The volume was calculated from the films' area and thickness, while the weight was measured using a laboratory sensitive four decimal weight balance. the density represented by calculating the average of 3 samples. The density is a result of dividing the film weight by the film volume:

$$\rho = \frac{m}{v} = g/cm^3 \quad (4)$$

where ρ = density; m = mass; and v = volume.

2.4.3. Moisture content (MC)

The weight loss of the film before and after drying the specimens at 90 °C for 24 h represents the moisture content, which was calculated for (3 × 1 cm) from the average of 3 replicates for each specimen according to:

$$MC = \frac{m1 - m2}{m1} X 100\% \quad (5)$$

where MC = water content, m1 = initial weight, and m2 = final weight.

2.4.4. Water solubility (WS)

After immersing the samples in 50 ml of distilled water for 6 h, water solubility was calculated. Then, the specimens were dried at 90 °C for 24 h and then weighed, *wi* in moisture content was the initial weight in water solubility. Water solubility was calculated using:

$$WS = \frac{wi - wf}{wi} X 100\% \quad (6)$$

Where

WS = water solubility: wi = initial dry weight, and wf = final dry weight.

2.4.5. Water absorption (WA)

The water absorption test was conducted according to ASTMD-570–98 standard [17]. The film specimens were dried for 24 h at 50 °C, cooled in a desiccator, and then directly weighed. After that, the samples were immersed in distilled

Table 1 – Mixtures designation of films-based treated and untreated fiber reinforced starch/PVA matrix.

Sample	Mixture designation				
	Starch (g)	Fructose (% of starch dry weight)	PVA (% of starch dry weight)	Fiber (% of starch dry weight)	Water (ml)
C	5	–	–	–	100
SPV0	5	35%	–	–	100
SPVA1	5	35%	25%	–	100
SP/3%TF	5	35%	25%	3% treated fiber	100
SP/6%TF	5	35%	25%	6% treated fiber	100
SP/9%TF	5	35%	25%	9% treated fiber	100
SP12%TF	5	35%	25%	12% treated fiber	100
SP/3%UTF	5	35%	25%	3% untreated fiber	100
SP/6%UTF	5	35%	25%	6% untreated fiber	100
SP/9%UTF	5	35%	25%	9% untreated fiber	100
SP/12%UTF	5	35%	25%	12% untreated fiber	100

water, and the weight was measured after 30 and 360 min. Water absorption was calculated according to:

$$WA = \frac{wf - wi}{wi} X100\% \quad (7)$$

WA = water absorption: wi = initial dry weight, and wf = final weight.

2.5. Film transparency

A spectrophotometer (BECKMAN COULTER/DU 730, Beckman Coulter, USA) was used to measure the opacity of each film to find out the transparency of each film. The transparency of each film was calculated according to:

$$\text{Opacity} = \frac{\text{Abs600}}{x} \quad (8)$$

where x represents the thickness (in mm) of the film, and Abs600 is the absorbance of light measured at 600 nm.

2.6. Biodegradation of biocomposites (soil burial test)

The biodegradation test was conducted by the method described by Ibrahim et al. [18]. Weight loss (WL) was measured in triplicate by obtaining samples at different times and cleaning them with a brush. The specimens were dried and weighed (wi) before being buried in 5 cm of soil in a restricted context (plastic boxes). Then, the weight of the samples was taken after being dehydrated for 6 h at 105 °C (Wf). The degradation test was performed on a weekly basis and the results were calculated by:

$$WL = \frac{wi - wf}{wi} X100\% \quad (9)$$

WL = weight loss: wi = initial dry weight and wf = final dry weight.

2.7. Simultaneous thermal analysis (STA)

STA test was carried out with a type of thermal properties analyzer (NETZSCH STA 449F3, Germany). Under a nitrogen environment, 10 mm^2 films were deposited in platinum crucibles and heated at a steady rate of 10 °C/min from RT to 500 °C. TGA curves were used to describe the thermal stability of samples and to assess mass loss over time as a function of temperature. DTG curves were used to describe the decomposition of distinct components of the composite.

2.8. Structural properties

2.8.1. Scanning electron microscopy (SEM)

To explore the surface morphology of the specimens, each specimen was coated with platinum coating before applying an acceleration voltage of 20 kV through a high vacuum using a JEOL- JSM-6010PLUS/LV and VPSEM CARL ZEISS EVO MA 10 (UK). This test yielded high-resolution photos at various magnification settings.

2.8.2. Fourier transform infrared spectroscopy (FTIR)

FTIR-ATr method was used to determine the FTIR spectra using the frequency range of 4000–650 cm^{-1}. The device model was an IR spectrometer Bruker Vector 22 IR spectrometer, Bruker, USA).

2.8.3. X-ray diffraction (XRD)

The XRD analysis was measured by an X-ray diffractometer (D8 ADVANCE | Bruker, Rigaku-Tokyo, Japan). The device was managed by 0.02 (θ) s^{-1} scattering speed within a 5–60° (2θ) angular range. Under operating voltage and current of 40 kV and 35 mA, respectively. According to:

$$Ci = \frac{Ac}{Ac + Aa} X100\% \quad (10)$$

Where:

Ci = crystallinity index, Ac = crystallinity area, and Aa = amorphous area in the XRD pattern.

2.9. Water vapor permeability (WVP)

Water vapor permeability was calculated from the water vapor transmission rate (WVTR) according to standard ASTM E96-00 [19]. Before starting the test, the films were put under 25 °C and 67% relative humidity for 48 h. During the test, the samples were placed over the mouth of the test cup prefilled with anhydrous calcium chloride. Then, the samples were placed under 25 °C and 75% relative humidity, following equations:

$$WVP = \frac{m \times t}{A \times T \times P} \quad (11)$$

$$WVTR = \frac{m}{A \times T} \quad (12)$$

$$WVP = \frac{WVTR}{P(R1 - R2)} \times t \quad (13)$$

Where:

WVP is water vapor permeability, WVTR is water-vapor transmission rate, t is film thickness (m), m is the weight increment of the cup (g), A is the area of the film that covers the cup mouth (m^2), T is the time lag for permeation (s), and P is water vapor partial pressure difference across the film (Pa). R1 is the RH in the desiccator, R2 is the RH in the cup, and t is the film thickness (m).

2.10. Tensile test

The tensile strength and modulus as well as elongation were determined using the ASTM-D882 standard [20]. Film strips were cut into 70 × 10 mm^2 sections. A tensile machine (UTM) (SHIMADZU/KUA 0400MED 00693, Japan) was used with a 500 N load. The initial grip separation and crosshead speeds were 30 mm and 1 mm/min, respectively. Five replicates were carried out for each sample. Before testing, all specimens were conditioned at RT in a desiccator for one week [21].

2.11. Statistical analyses

The statistical analyses of the experimental results were analyzed using Microsoft Excel 2016.

3. Results

3.1. Physical properties

3.1.1. Thickness and density

The addition of fructose has increased the film thickness, C, and SPV0 films resulted from casting 22 g in 90 mm dishes, while the rest of the samples resulted from casting 15 g. Generally, the addition of fiber increased the thickness, films reinforced with treated fiber showed lower thickness than films reinforced with untreated fiber. While alkaline treatment has been shown to increase fiber density, it also increases the density of the biopolymer, which is why biofilms filled with treated fiber have a higher density than those filled with untreated fiber [22]. When the fiber was added to a matrix made of starch and PVA, an intermolecular interaction occurs between the fiber and the polymer matrix. Thicker and coarser films were produced as a result of the increased fiber content, which increases porosity and produces a less uniform structure with a lower density than thermoplastic starch [23,24]. The reinforced film showed high density at a 3% fiber load in both treated and untreated fibers. The increment in fiber content resulted in more porosity and a less uniform structure with a lower density than thermoplastic starch, resulting in thicker and coarser sheets. However, this significant reduction in density, lighter weight bioplastic was produced as the density of the polymer decreased to 1.21 g/cm^3 with untreated fibers and to 1.32 g/cm^3 with treated fibers. This Makes the biopolymer more attractive in many different applications that require low-weight polymers.

3.1.2. Moisture content (MC), water solubility (WS) and water vapor permeability (WVP)

The features of the film particles interacting with water, such as moisture content and water solubility are key qualities for applications that need specified moisture content and insolubility. As shown in Table 2, the addition of fructose and PVA reduced the moisture content, while the addition of fiber increased it. SP12%TF and SP/9%UTF showed low moisture content compared to other reinforced films. For water solubility, the film produced from pure starch showed the lowest water solubility (2.54%), while the solubility increased with the addition of fructose and PVA. The addition of fiber has effectively reduced the water solubility, most of the samples revealed a significant reduction in water solubility after adding treated or untreated fiber, the enhancement was around (17.54–29.72%). Those findings agreed with the findings of [18].

Reinforcing the starch-PVA matrix with fiber has considerably improved WVP resistance, reinforcing the matrix with treated fiber improved the resistance of WVP to untreated fiber. However, the improvement in WVP resistance occurred gradually with the addition of palm fiber. SP/9%TF, SP/12%TF, and SP/12%UTF demonstrated 1.09, 1.01, and 1.03 10^{-10}g.mm. S^{-1} m^{-2} Pa^{-1}, respectively, making them less vapor permeable when compared with the first control film. The hydrophilic nature of starch, fructose, and PVA is the main reason for the WVP of their films [25]. The reduction in WVP could be due to the creation of a stiff crystalline structure and a high dispersion of fiber particles in the biopolymer matrix, which obstructed the WVP path [26]. Increased intermolecular interaction between the CS-matrix and SPF-reinforcement, which minimized or eliminated matrix chain mobilization, is another possible explanation for the observed behavior.

3.1.3. Water absorption

Water is important in biopolymers because it acts as a plasticizer, allowing the material to be more flexible. Based on the result in Table 2, the first reduction in the absorbed water amount was founded with the addition of fructose, while the addition of PVA declined this enhancement back to 208.5% after 6 h. Reinforcing matrix film with palm fiber has improved water resistance properly. In the case of treated fiber, reinforcing the matrix with 3% of treated fiber gave the highest water resistance. Also, it has been found that higher amounts of fiber reduce water resistance. Nevertheless, untreated fiber showed the highest water resistance at 12% of untreated fiber load. The increment in water absorption in a certain amount of fiber can be attributed to the hydrophilic behavior of both treated and untreated fibers [27]. When a particular fiber load

Table 2 – Physical properties of films-based treated and untreated fiber reinforced starch/PVA matrix.

Blend	Thickness μm	Density g/cm^3	MC %	WS %	WVP 10^{-10}g.mm .s^{-1} m^{-2} Pa^{-1}	Crystalli-nity index (%)	WA% 30 min	WA% 360 min	Opacity (A600/mm)
C	170.2	1.32	11.86	2.54	1.12	18.90	334.58	467.15	0.808
SPV0	200.2	1.39	9.15	29.02	1.53	16.90	150.24	187.42	0.624
SPVA1	150.0	1.39	9.17	30.95	2.67	21.63	179.39	208.48	1.924
SP/3%TF	198.0	1.61	12.26	24.93	1.23	37.28	142.99	159.47	2.240
SP/6%TF	202.0	1.48	12.97	24.53	1.18	38.05	174.47	188.81	2.136
SP/9%TF	206.0	1.36	11.35	21.75	1.09	49.82	179.22	196.58	1.958
SP12%TF	216.0	1.32	10.84	24.97	1.01	43.31	171.13	191.06	2.670
SP/3% UTF	172.0	1.56	10.86	25.52	1.72	39.02	177.28	200.50	1.971
SP/6% UTF	196.0	1.35	11.29	25.13	1.24	34.83	181.72	194.65	2.887
SP/9% UTF	214.0	1.31	9.21	24.03	1.13	48.77	177.01	200.22	3.227
SP/12% UTF	240.0	1.21	10.24	23.52	1.03	44.18	158.01	192.30	3.307

reduced water resistance, the starch matrix's porosity increased, leading to an increase in water diffusion.

3.2. *Structural properties*

3.2.1. *Scanning electronic microscopy (SEM)*

Two magnifications were applied to show the morphological structure, 300× for unreinforced matrix and 40X for reinforced matrix. Control and SPV0 film showed smooth surfaces with some cracks, while PVA addition showed macro cracks and voids. The existence of treated and untreated can be easily observed in the hybrid matrix. The existence of treated and untreated sugar palm fiber can be easily observed in the hybrid matrix. The presence of the fiber is sometimes detected close to the surface, as with SP/3%TF and SP/12%UTF, and sometimes not, as with SP/6%TF and SP/6%UTF.it didn't always happen in an individual form; occasionally, it produced small aggregates instead [28]. As displayed in Fig. 1, the addition of fiber generally has created a stiff, non-uniform, and rough texture surface. Fig. 1 also illustrated that 6% of

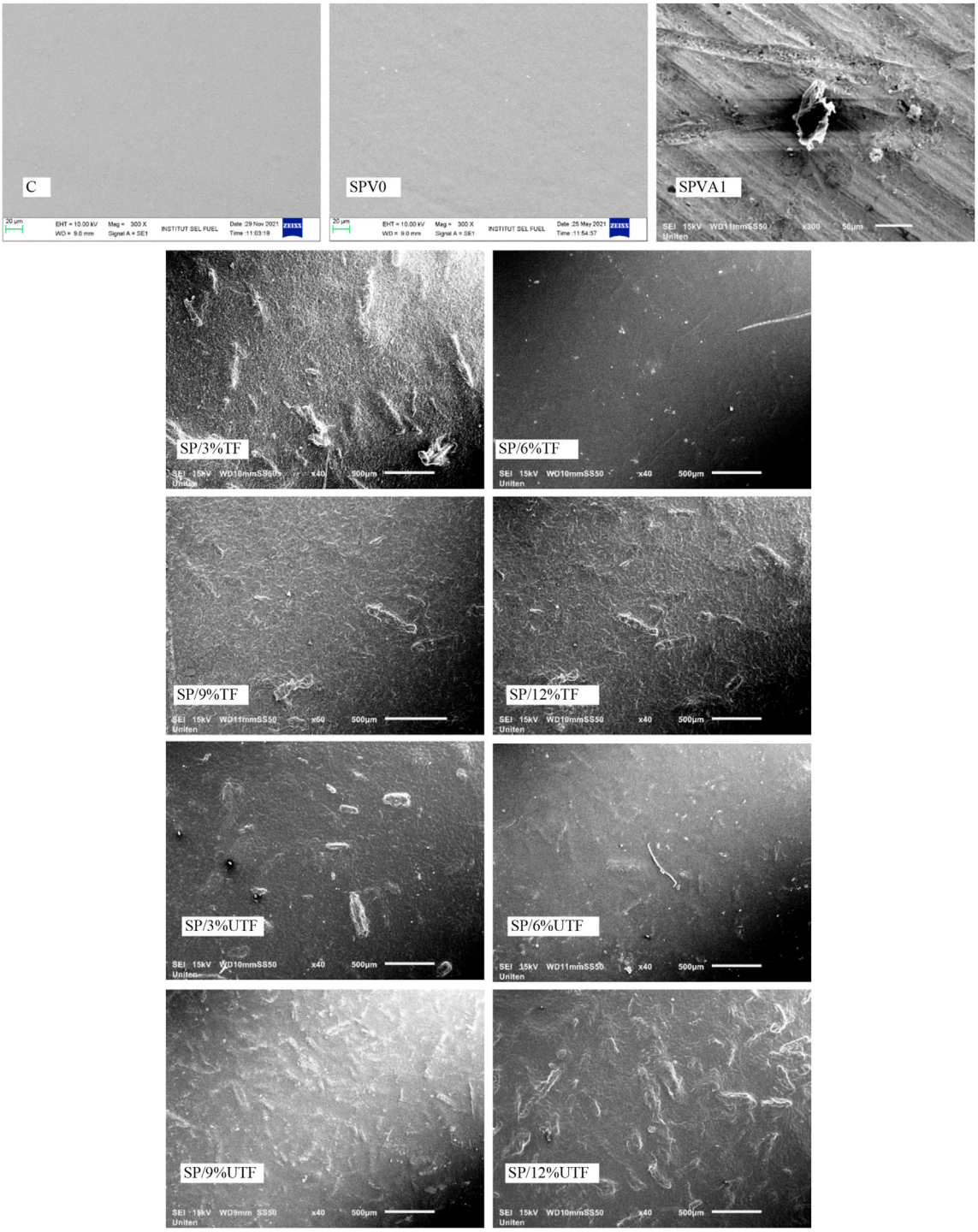

Fig. 1 – SEM images of films based treated and untreated fiber reinforced starch/PVA matrix.

both treated and untreated fiber loads demonstrated higher compatibility between fiber and matrix. Fiber particles that acted as a nucleation agent for crystal formation were responsible for the rise in crystallinity as a result of the nucleation effects that the addition of fibers created.

3.2.2. *Fourier transform infrared (FT-IR) spectroscopy*

FT-IR test was applied to determine the interaction of bioplastic in different stages, starting from the control film without any fiber addition. This is to study the effect of adding 35% fructose-based starch weight, 25% PVA-based starch weight, and the treated and untreated palm fibers. Fig. 2 showed almost similar curves because of the almost similar elemental composition of the plasticized films since the main structure of the polymer is the starch.

The peak observed in 3280.07 cm^{-1} referred to stretching of the O–H groups [29], which can be detected in general the range of 3550 cm^{-1} -3200 cm^{-1}, this peak shifted to less wavenumber with the addition of fructose, while this peak escalated to higher wavenumber by adding PVA. At 2924.46 cm^{-1}, in the range of 3000 cm^{-1} -2840 cm^{-1} a sharp peak attributed to the C–H group [30] was detected, 1635.43 cm^{-1} peak referred to the bending mode of the absorbed water [31]. A peak at 1337.94 cm^{-1} was a sign of CH_2 bonding [32], 1149.45 cm^{-1} sharp peak was a sign of the coupling of C–C and C–O stretching mode [33], 1076.98 cm^{-1} peak is ascribed to C–O–H group in wheat starch [34], indicating crystal modification of the starch structure [35], and 994.13 cm^{-1} peak denoting C–O stretching in C–O–C and C–O–H in the glycosidic ring of starch and lignin [36–38]. The 860.35 cm^{-1} peak indicated strong C–H bending [39] and 759.70 cm^{-1} peak represented the vibrations of the glucose pyranose unit [40], in general, this peek can be found in the range of 770 cm^{-1} -735 cm^{-1}. There was no difference in terms of adding treated and untreated palm fiber, both of them showed similar behavior. In the aspect of shifting to a higher wavenumber in hydrogen bonding, this peak was higher in the control film since there were no any additions. The addition of fructose shifted it back to 3255.65 cm^{-1} while the addition of PVA improved the hydrogen bonding significantly,

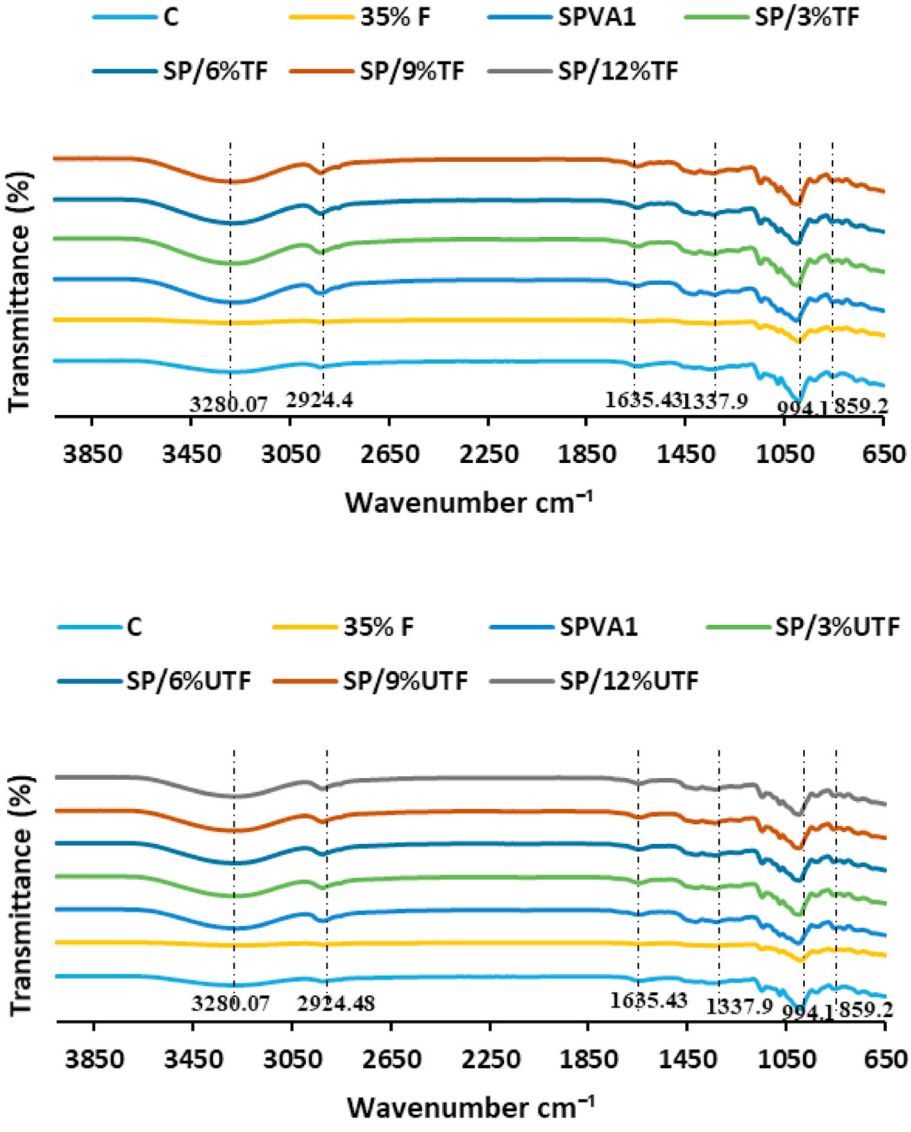

Fig. 2 – FT-IR curves of films-based treated and untreated fiber reinforced starch/PVA matrix.

Table 3 – Frequent ranges for IR spectrum that occurred in this study [41,42].

Absorption (cm^{-1})	Comment
3550–3200	Strong, broad O–H stretching
3000–2840	Medium C–H stretching
1650–1500	Absorbed water
1368–1333	CH_2 bonding
1085–1150	Strong C–O stretching
1182–1157	C–O–H group in wheat starch
1020–988	C–O stretching in C–O–C and C–O –H in the glycosidic ring of starch and lignin
900–859	Strong C–H bending
860–800	Strong C–H bending
770–735	Vibrations of glucose pyranose unit

reaching 3270.85 cm^{-1} that indicating higher intermolecular hydrogen bonding between starch and PVA. This increment was also improved with the addition of treated and untreated fibers. However, this increment was not in a linear pattern, it kept increasing at SP/6%TF until it reached 3274.27 cm^{-1}. More loading of fiber reduced the wavenumber of this peak at SP/9% TF while it showed a slight increase at SP/12%TF. On the other hand, untreated fiber showed frequent increasing, the higher wavenumber of hydrogen bonding occurred at SP/3%UTF and SP/9%UTF resulted in 3273 cm^{-1} while it was 3272 cm^{-1} at SP/ 6%UTF and SP/12%UTF. Table 3 summarizes the ranges of detected peaks in this work.

3.2.3. *X-ray diffraction (XRD)*

XRD test was conducted to study the crystal structure of the biopolymers produced from wheat starch, fructose, PVA, and palm fiber. As the result presented in Table 2, the addition of treated and untreated fibers has considerably improved the crystallinity index of the biopolymer. Reinforcing the matrix with 9% of either treated or untreated fiber exhibited the highest crystallinity index, it reached 49.8 and 48.7, respectively. The internal structure of composites grew less amorphous and more ordered when the starch particles penetrated the pores of the fiber, phase separation between fiber and starch is what causes the growing trend in the crystallinity of fiber reinforcement composites [43].

The control film had sharp diffraction peaks located at $2\theta = 15.08°$, $2\theta = 17.32°$, and $2\theta = 19.44°$. SPV0 film showed two distinguished peaks at $2\theta = 17.12°$ and $2\theta = 19.44°$, the low degree of the peaks due to the low crystallinity index [44]. The addition of PVA hasn't change the XRD profile significantly, nevertheless, the peaks get to be sharper and intense with the addition of PVA. With the addition of fibers, sharper and more intense peaks were observed as shown in Fig. 3. The reason for this is the nucleation effects, in which fiber particles that worked as a nucleation agent for crystal growth were responsible for the increase in crystallinity [45].

3.3. *Simultaneous thermal analysis (STA)*

STA test was used to measure the thermal stability of the bioplastic by monitoring the weight change that occurred as a sample was heated at a predetermined heating rate [46]. Fig. 4 shows TGA and DTG curves of the films-based treated and untreated fiber reinforced starch/PVA matrix. DTG curve of control film to phases peaks at 122.1 and 298.6 °C attributed to moisture removal and starch degradation, respectively. The addition of fructose and PVA revealed two more peaks 225.5 and 421 °C referring to the decomposition of fructose and PVA, respectively. The main structure, on the other hand, showed remarkable thermal stability since the starch structure decomposed at 302.3 °C. Fig. 5 shows the mass residues at 495 °C of various films. The reason why untreated fiber film showed higher mass residues was that untreated fiber had a higher amount of lignin as shown in the graphical abstract. The lignin structure has a higher decomposition temperature than cellulose and hemicellulose according to [47] who reported the thermal breakdown of lignocellulose plant fiber

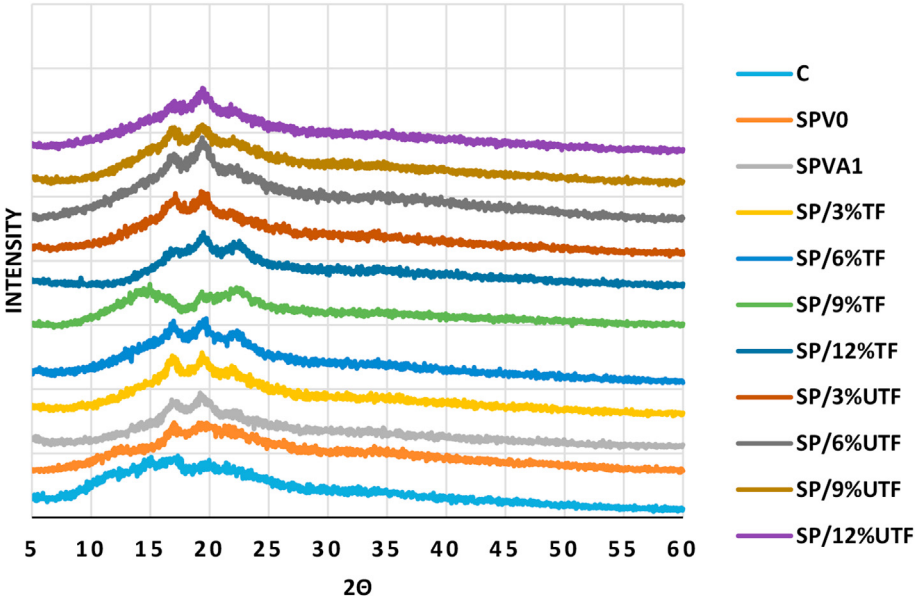

Fig. 3 – XRD curves of films-based treated and untreated fiber reinforced starch/PVA matrix.

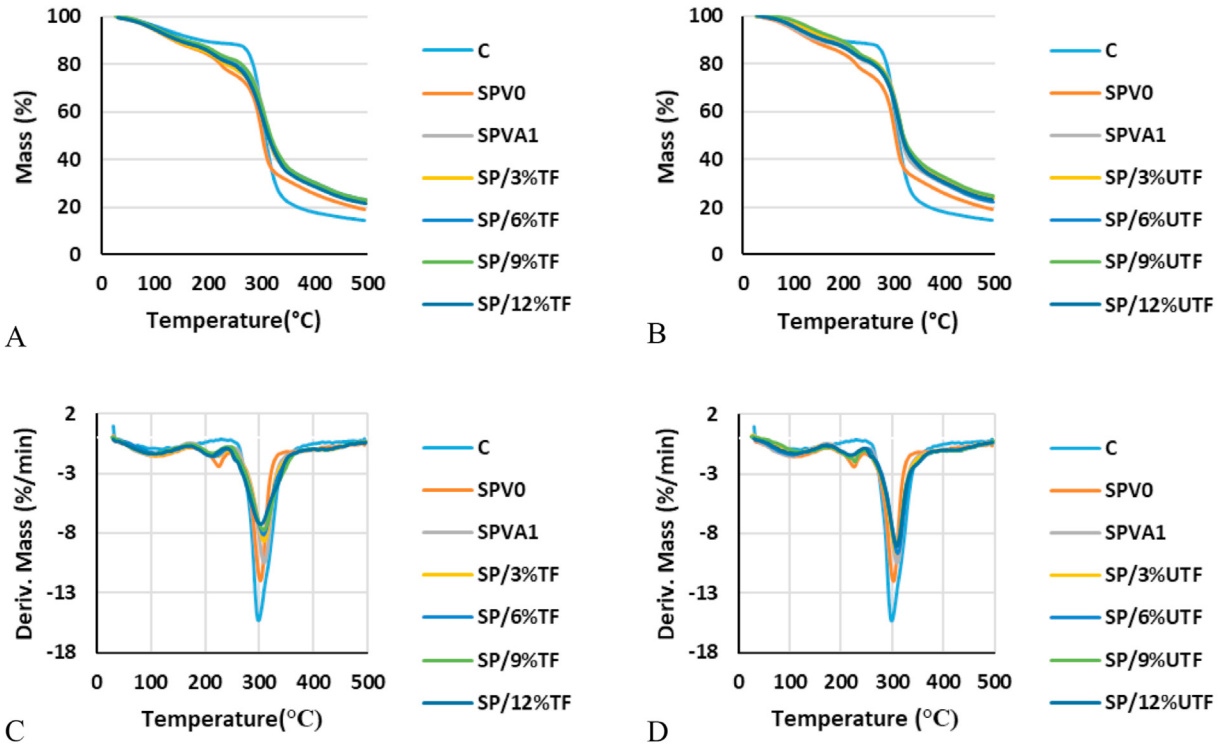

Fig. 4 – TGA and DTG curves of films-based treated and untreated fiber reinforced starch/PVA matrix. A), C) treated fiber, and B), D) untreated fiber.

that begins with the disintegration of hemicellulose at temperatures ranging from 200 to 260 °C, cellulose at 240–350 °C, and lignin at 280–500 °C, depending on the plant species and fabric component percentages. 9% of fiber load demonstrated higher thermal stability for both treated and untreated fibers, SP/9%TF and SP/9%UTF revealed 23.3% and 24.6% mass residues, respectively. TGA chart shows a significant enhancement with the addition of fiber compared to C, SPV0, and SPVA1 samples. This enhancement occurred after 312 °C, where samples reinforced with fiber showed higher resistance towards thermal decomposition than samples without fiber.

3.4. *Soil degradation*

In order to measure the decomposition of biofilm in soil, the weight of samples was measured weekly. As presented in Fig. 6, C and SPV0 films were both fully degraded within two weeks, whilst adding PVA has reduced the degradation significantly. On the other hand, reinforcing the starch-PVA

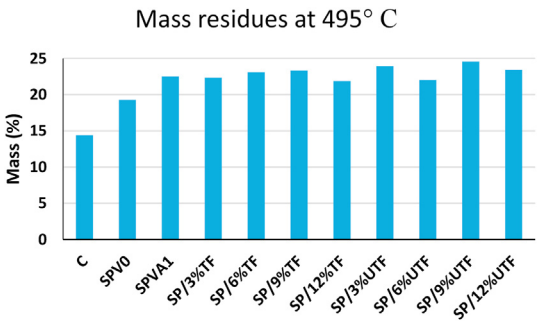

Fig. 5 – Mass residues at 495 °C of films based treated and untreated fiber reinforced starch/PVA matrix.

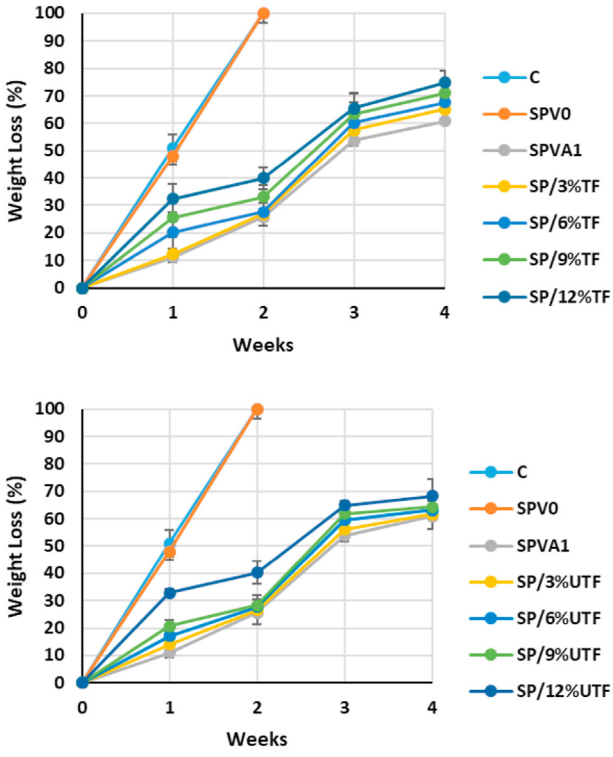

Fig. 6 – Soil degradation of films based treated and untreated fiber reinforced starch/PVA matrix.

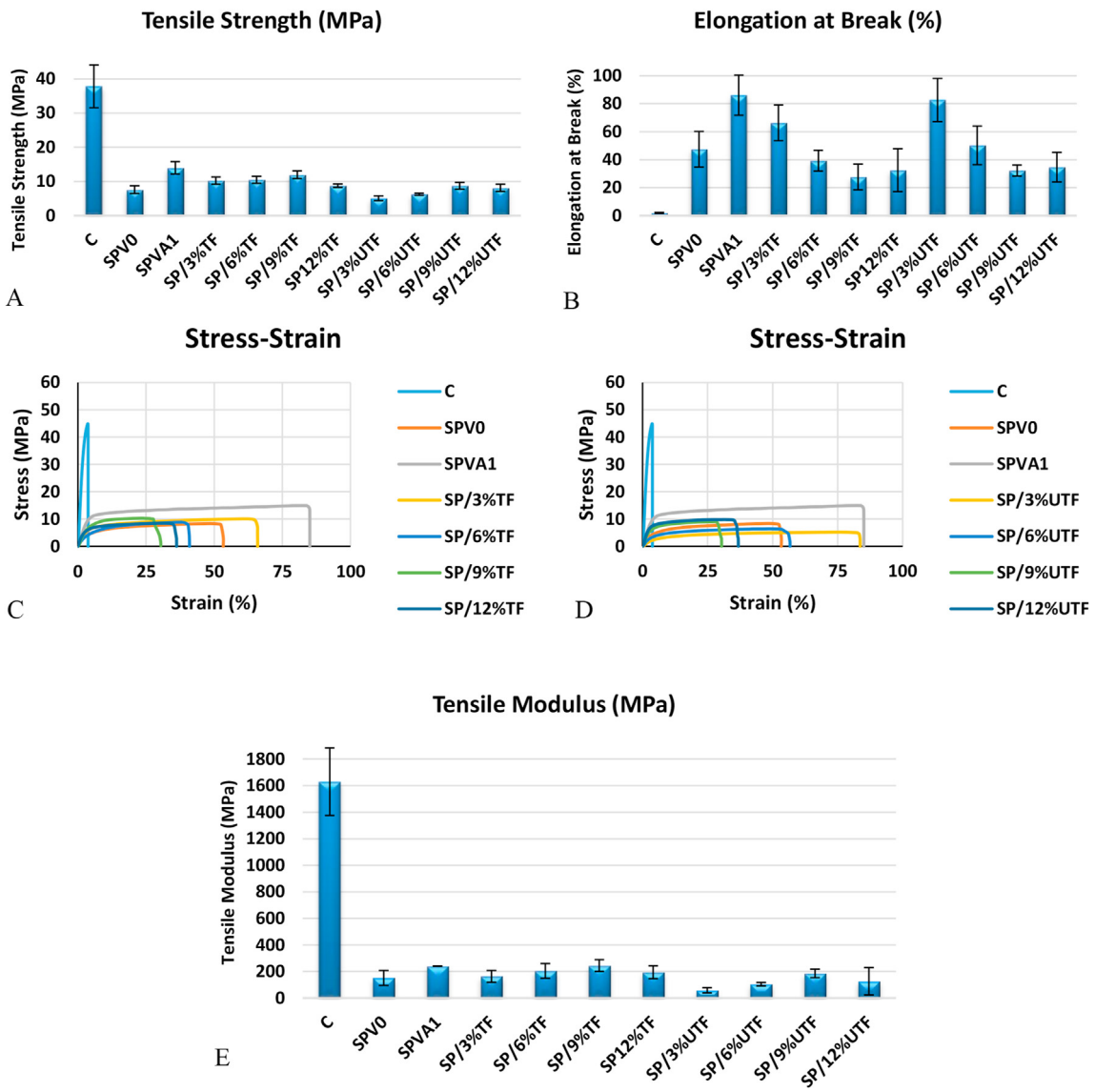

Fig. 7 – Mechanical properties of films-based treated and untreated fiber reinforced starch/PVA matrix. A) Tensile strength, B) Elongation at break, C) Stress-Stain chart for films filled with treated fiber, D) Stress-Stain chart for films filled with untreated and E) tensile modulus.

matrix with palm fiber has improved the biofilm degradation compared to the net starch-PVA film, while treated fiber resulted in a higher degradation rate than untreated fiber. For instance, at 12% fiber load, the weight loss of treated fiber films was 75% in the fourth week, while it was 68% for untreated fiber. According to the results, the film with higher fiber content has a higher potential for decomposition in soil, making it more vulnerable to mycobacterial attack. In the presence of an aqueous media, this microorganism, in the form of fungi and bacteria, impacts the composite films [18].

3.5. *Film transparency*

The value of film transparency varies depending on the application; generally, film transparency is very desirable in food packaging applications. Opacity is a word used to represent the polar opposite of film transparency, which takes into consideration the thickness of the film.

The addition of fructose has significantly improved the transparency, inversely, PVA addition reduced it. Treated fiber showed similar opacity to the SPVA1 sample with 9% fiber, while other loads of treated fiber escalated the opacity. The untreated fiber showed this phenomenon at 3% load. Higher opacity was recorded for SP/12%UTF. Table 2 shows the effect of treated and untreated fiber on the films obtained. Generally, samples based on untreated fiber are more opaque than treated fiber, whereas treated fiber which mostly consists of cellulose has higher opacity than starch [48]. That is the reason fiber addition in biofilms has never overcome the transparency of the film without fiber.

3.6. *Tensile test*

In order to determine the usefulness of a material, it's important to study its tensile behavior. Fig. 7 shows that with highest tensile and modulus values for the control film were

38 and 1630 MPa, respectively. At the break, it had the lowest elongation (1.94%). In the case of plasticized films, plasticizing wheat starch with 35% fructose showed a reduction in tensile strength and modulus, while it improved the elongation at break, whilst adding PVA improved the tensile strength, modulus, and elongation at break. In all samples, water was frequently used as the main plasticizer because of its capacity to hydrolyze the molecular link structure of starch when heated together [49].

Reinforcing the SPVA1 matrix with treated palm fiber showed a slight reduction in tensile strength, modulus, and elongation. However, improvements in tensile strength and modulus occurred at 9% of treated fiber load, showing 12 MPa and 245 MPa, respectively. The highest elongation was 66.3% at 3% of treated fiber films. On the other hand, untreated fiber films showed lower tensile strength and modulus in all loads, whereas, 3% of untreated fiber films recorded 82% of elongation at break, which is considered higher than the treated fiber films. In terms of increase in tensile, untreated and treated fiber films showed comparable behavior where the highest tensile strength and modulus for untreated fiber films were gained at 9% of untreated fiber, which were 8.7 and 186 MPa, respectively.

The cause of the lower tensile in untreated fiber film was due to the creation of voids inside the polymer matrix, which resulted in cracks at the biocomposite interface [50]. While the general reduction of tensile in both treated and untreated fiber film can be attributed to the aggregation of fiber particles [51] and the fiber particles' size themselves. The highest aggregation happened with the untreated fiber due to the availability of surface hydroxyl groups in the fiber [52], which was reduced by the fiber treatment. In this study, the addition of PVA improved the polymer stiffness and elongation, making it difficult for further improvement in the tensile properties without losing the privilege of good elongation. Fig. 7 also shows the reduction in strain with the addition of fiber content.

4. Conclusions

The use of biodegradable polymers from agricultural sources is particularly promising from the standpoint of the circular economy and sustainable development. In order to increase flexibility of biopolymers based-starch, plasticizers such fructose is utilized. Improved mechanical qualities can be achieved by synthesizing polymers like polyvinyl alcohol (PVA), which is an excellent approach in general. Natural fibers reinforcement of bio-matrix has a considerable positive impact. Reinforcing starch/PVA-based matrix has revealed significant improvement, the biopolymers become more resistant to water uptake with lower weight, more thermal stability, and more crystal profile. While mechanical properties were reduced with the addition of fiber, however, these reductions were less than the amount with the addition of treated fiber. SP/9%TF showed the best average mechanical properties compared to reinforced samples (tensile strength, modulus, and elongation at break, which were 12 MPa, 245 MPa, and 27.6%, respectively). Some films showed low tensile properties, for example, SP/3%UTF resulted in 5 MPa as tensile strength. Generally, for both treated and untreated fiber, 9% load gave the highest tensile properties. SEM images revealed more compatibility between fiber and matrix at 9% fiber load, which illustrated the properties improvement at this point.

Author contributions

Conceptualization, Abdulrahman A. B. A. Mohammed, Abdoulhdi A. Borhana Omran, R.A. Ilyas and S. M. Sapuan; Formal analysis, Abdulrahman A. B. A. Mohammed, Zaimah Hasan, Abdoulhdi A. Borhana Omran, Abdulhafid M Elfaghi, Yasir Hassan Ali, R.A. Ilyas and S. M. Sapuan; Funding acquisition, Zaimah Hasan and Abdoulhdi A. Borhana Omran; Investigation, Abdulrahman A. B. A. Mohammed and Abdoulhdi A. Borhana Omran; Methodology, Abdulrahman A. B. A. Mohammed, Abdoulhdi A. Borhana Omran, R.A. Ilyas and S. M. Sapuan; Project administration, Abdoulhdi A. Borhana Omran, R.A. Ilyas and S. M. Sapuan; Resources, Zaimah Hasan and Abdoulhdi A. Borhana Omran; Supervision, Zaimah Hasan and Abdoulhdi A. Borhana Omran; Visualization, Abdulrahman A. B. A. Mohammed; Writing – original draft, Abdulrahman A. B. A. Mohammed and Abdoulhdi A. Borhana Omran; Writing – review & editing, Abdulrahman A. B. A. Mohammed, Zaimah Hasan, Abdoulhdi A. Borhana Omran, Abdulhafid M Elfaghi, Yasir Hassan Ali, R.A. Ilyas and S. M. Sapuan.

Funding

Authors are thankful to Universiti Tenaga Nasional (UNITEN), Malaysia for providing financial supports for this study under BOLD Publication Fund 2022 (J510050002 - IC-6 BOLDREFRESH2025 - CENTRE OF EXCELLENCE), BOLD2020 grants coded J51005000/2021014 and BOLD2020 grant coded J51005000/2021073 by Innovation & Research Management Center (iRMC), Universiti Tenaga Nasional, Malaysia.

Declaration of Competing Interest

The authors declare that they have no known competing financial interests or personal relationships that could have appeared to influence the work reported in this paper.

Acknowledgments

Authors are thankful to Universiti Tenaga Nasional (UNITEN), Malaysia for providing financial supports for this study under BOLD Publication Fund 2022 (J510050002 - IC-6 BOLDREFRESH2025 - CENTRE OF EXCELLENCE), BOLD2020 grants coded J51005000/2021014 and BOLD2020 grant coded J51005000/2021073 by Innovation & Research Management Center (iRMC), Universiti Tenaga Nasional, Malaysia.

REFERENCES

[1] Mohammed AABA, Omran AAB, Hasan Z, Ilyas RA, Sapuan SM. Wheat biocomposite extraction, structure, properties and characterization: a review. Polymers 2021;13(21):3624. https://doi.org/10.3390/polym13213624.

[2] Ibrahim NI, Shahar FS, Sultan MT, Shah AU, Safri SN, Mat Yazik MH. Overview of bioplastic introduction and its applications in product packaging. Coatings 2021;11(11). https://doi.org/10.3390/coatings11111423.

[3] Porta R, Sabbah M, Di Pierro P. Bio - based materials for packaging. 2022. p. 1–5.

[4] Mohammed Abdulrahman ABA, Hasan Zaimah, Omran Abdoulhdi A Borhana, Elfaghi Abdulhafid M, Khattak MA, Ilyas RA, et al. Effect of various plasticizers in different concentrations on physical, thermal, mechanical, and structural properties of wheat starch-based films. Polymers 2023;15(1). https://doi.org/10.3390/polym15010063.

[5] Kasim A. Improvement on the bioplastic properties of polyvinyl alcohol (PVA) with the sago starch nanoparticle addition. SYLWAN 2022;166(1):130.

[6] Quintaliani C, Merli F, V Fiorini C, Corradi M, Speranzini E, Buratti C. Vegetal fiber additives in mortars: experimental characterization of thermal and acoustic properties. Sustainability 2022;14(3). https://doi.org/10.3390/su14031260.

[7] Shevkani K, Singh N, Bajaj R, Kaur A. Wheat starch production, structure, functionality and applications—a review. Int J Food Sci Technol 2017;52(1):38–58. https://doi.org/10.1111/ijfs.13266.

[8] Martens BMJ, Gerrits WJJ, Bruininx EMAM, Schols HA. Amylopectin structure and crystallinity explains variation in digestion kinetics of starches across botanic sources in an in vitro pig model. J Anim Sci Biotechnol 2018;9(1):91. https://doi.org/10.1186/s40104-018-0303-8.

[9] Tian H, Yan J, Rajulu AV, Xiang A, Luo X. Fabrication and properties of polyvinyl alcohol/starch blend films: effect of composition and humidity. Int J Biol Macromol 2017;96:518–23. https://doi.org/10.1016/j.ijbiomac.2016.12.067.

[10] Patra N, Salerno M, Cernik M. 22 - electrospun polyvinyl alcohol/pectin composite nanofibers. In: Afshari MBT-EN, editor. Woodhead publishing Series in textiles. Woodhead Publishing; 2017. p. 599–608.

[11] Omran Abdoulhdi A Borhana, Mohammed Abdulrahman ABA, Sapuan SM, Ilyas RA, Asyraf MRM, Koloor Seyed Saeid Rahimian, et al. Micro- and nanocellulose in polymer composite materials: a review. Polymers 2021;13(2). https://doi.org/10.3390/polym13020231.

[12] Mohammed Abdulrahman ABA, Hasan Zaimah, Omran Abdoulhdi A Borhana, Kumar V Vinod, Elfaghi Abdulhafid M, Ilya RA, et al. Corn: its structure, polymer, fiber, composite, properties, and applications. Polymers 2022;14(20). https://doi.org/10.3390/polym14204396.

[13] "Products: Starches – Bestari Food Malaysia." [Online]. Available: https://www.bestarifood.com/products-starches/. [Accessed: 03-September-2022].

[14] Gomaa WMS, Mosaad GM, Yu P. On a molecular basis, investigate association of molecular structure with bioactive compounds, anti-nutritional factors and chemical and nutrient profiles of canola seeds and Co-products from canola processing: comparison crusher plants within Canada and. Nutrients 2018;10(4). https://doi.org/10.3390/nu10040519.

[15] Coelho Caroline Corrêa de Souza, Silva Raysa Brandão Soares, Carvalho Carlos Wanderlei Piler, Rossi André Linhares, Teixeira José António, Freitas-Silva Otniel, et al. Cellulose nanocrystals from grape pomace and their use for the development of starch-based nanocomposite films. Int J Biol Macromol 2020;159:1048–61. https://doi.org/10.1016/j.ijbiomac.2020.05.046.

[16] Lu Y, Weng L, Cao X. Morphological, thermal and mechanical properties of ramie crystallites - reinforced plasticized starch biocomposites. Carbohydr Polym 2006;63(2):198–204. https://doi.org/10.1016/j.carbpol.2005.08.027.

[17] ASTM D570, "Standard test method for water absorption of plastics," ASTM Stand., vol. 98, no. Reapproved 2010, pp. 25–28, 2014, https://doi.org/10.1520/D0570-98R18.2.

[18] Ibrahim MIJ, Sapuan SM, Zainudin ES, Zuhri MYM. Potential of using multiscale corn husk fiber as reinforcing filler in cornstarch-based biocomposites. Int J Biol Macromol 2019;139:596–604. https://doi.org/10.1016/j.ijbiomac.2019.08.015.

[19] Standard Test Methods for Water Vapor Transmission of Materials." [Online]. Available: https://www.astm.org/e0096-00.html. [Accessed: 28-Jan-2023].

[20] Standard Test Method for Tensile Properties of Thin Plastic Sheeting." [Online]. Available: https://www.astm.org/d0882-18.html. [Accessed: 28-Jan-2023].

[21] Lv C, Tian H, Zhang X, Xiang A. LF-NMR analysis of the water mobility, state and distribution in sorbitol plasticized polyvinyl alcohol films. Polym Test 2018;70:67–72. https://doi.org/10.1016/j.polymertesting.2018.06.024.

[22] Bekele AE, Lemu HG, Jiru MG. Experimental study of physical, chemical and mechanical properties of enset and sisal fibers. Polym Test 2022;106:107453. https://doi.org/10.1016/j.polymertesting.2021.107453.

[23] Versino F, García MA. Cassava (Manihot esculenta) starch films reinforced with natural fibrous filler. Ind Crop Prod Jul. 2014;58:305–14. https://doi.org/10.1016/j.indcrop.2014.04.040.

[24] Begum MHA, Hossain MM, Gafur MA, Kabir ANMH, Tanvir NI, Molla MR. Preparation and characterization of polyvinyl alcohol–starch composites reinforced with pulp. SN Appl Sci 2019;1(9):1091. https://doi.org/10.1007/s42452-019-1111-2.

[25] Gaudin S, Lourdin D, Forssell P, Colona P. Antiplasticisation and oxygen permeability of starch-sorbitol films. Carbohydr Polym Sep 2000;43:33–7. https://doi.org/10.1016/S0144-8617(99)00206-4.

[26] Slavutsky AM, Bertuzzi MA. Water barrier properties of starch films reinforced with cellulose nanocrystals obtained from sugarcane bagasse. Carbohydr Polym 2014;110:53–61. https://doi.org/10.1016/j.carbpol.2014.03.049.

[27] Boonsuk P, Sukolrat A, Chantarak S, Kelarakis A, Chaibundit C. Poly(vinyl alcohol)/modified cassava starch blends plasticized with glycerol and sorbitol. J Appl Polym Sci Mar 2022:52362. https://doi.org/10.1002/app.52362. vol. n/a, no. n/a.

[28] Wittaya T. Microcomposites of rice starch film reinforced with microcrystalline cellulose from palm pressed fiber. Int Food Res J 2009;16(4):493–500.

[29] Lee CM, Kubicki JD, Fan B, Zhong L, Jarvis MC, Kim SH. Hydrogen-bonding network and OH stretch vibration of cellulose: comparison of computational modeling with polarized IR and SFG spectra. J Phys Chem B 2015;119(49):15138–49. https://doi.org/10.1021/acs.jpcb.5b08015.

[30] Trivedi MK, Dahryn Trivedi AB, Khemraj Bairwa HS. Fourier transform infrared and ultraviolet-visible spectroscopic characterization of biofield treated salicylic acid and sparfloxacin. Nat Prod Chem Res 2015;3(5). https://doi.org/10.4172/2329-6836.1000186.

[31] Seki Takakazu, Chiang Kuo-Yang, Yu Chun-Chieh, Yu Xiaoqing, Okuno Masanari, Hunger Johannes, et al. The bending mode of water: a powerful probe for hydrogen bond structure of aqueous systems. J Phys Chem Lett Oct.

2020;11(19):8459–69. https://doi.org/10.1021/acs.jpclett.0c01259.
[32] Jaafar J, Siregar JP, Oumer AN, Hamdan MHM, Tezara C, Salit MS. Experimental investigation on performance of short pineapple leaf fiber reinforced tapioca biopolymer composites. Bioresources 2019;13(3):6341–55. https://doi.org/10.15376/biores.13.3.6341-6355.
[33] Corsetti S, Zehentbauer FM, McGloin D, Kiefer J. Characterization of gasoline/ethanol blends by infrared and excess infrared spectroscopy. Fuel 2015;141:136–42. https://doi.org/10.1016/j.fuel.2014.10.025.
[34] Orphanou CM. The detection and discrimination of human body fluids using ATR FT-IR spectroscopy. Forensic Sci Int 2015;252:e10–6. https://doi.org/10.1016/j.forsciint.2015.04.020.
[35] Jacob, J., Gomes, F., Haponiuk, J.T., Kalarikkal, N., & Thomas, Natural polymers: perspectives and applications for a green approach (1st ed.). Apple Academic Press. https://doi.org/10.1201/9781003130765.
[36] Horikawa Y, Hirano S, Mihashi A, Kobayashi Y, Zhai S, Sugiyama J. Prediction of lignin contents from infrared spectroscopy: chemical digestion and lignin/biomass ratios of cryptomeria japonica. Appl Biochem Biotechnol Aug. 2019;188. https://doi.org/10.1007/s12010-019-02965-8.
[37] Jae Gyoung G, Lee S, Doh G, Kim J. Characterization of chemically modified wood fibers using FTIR spectroscopy for biocomposites. J Appl Polym Sci Jun 2010;116:3212–9. https://doi.org/10.1002/app.31746.
[38] Yaacob B, Amin MCIM, Hashim K, Bakar BA. Optimization of reaction conditions for carboxymethylated sago starch. Iran Polym J (English Ed) 2011;20(3):195–204.
[39] Naznin M, Abedin MZ. Effect of sugar, urea, and molasses and the influence of radiation on the plasticization of Acacia catechu extract incorporated starch/poly-(vinyl alcohol) based film. ISRN Polym Sci. 2013;2013:1–10. https://doi.org/10.1155/2013/593862.
[40] Flores-Morales A, Jiménez-Estrada M, Mora-Escobedo R. Determination of the structural changes by FT-IR, Raman, and CP/MAS 13C NMR spectroscopy on retrograded starch of maize tortillas. Carbohydr Polym Jan 2012;87:61–8. https://doi.org/10.1016/j.carbpol.2011.07.011.
[41] IR Spectrum Table." [Online]. Available: https://www.sigmaaldrich.com/MY/en/technical-documents/technical-article/analytical-chemistry/photometry-and-reflectometry/ir-spectrum-table. [Accessed: 22-November-2021].
[42] Ogunmolasuyi AM, Egwim EC, Adewoyin MA, Nkop EJ. Physicochemical and structural characterization of yam starch modified by potassium dihydrogen phosphate treatment in aqueous glycerol. Edorium J Biotechnol 2016;2(May):6–14. https://doi.org/10.5348/B08-2016-3-OA-2.
[43] Ma X, Yu J, Kennedy JF. Studies on the properties of natural fibers-reinforced thermoplastic starch composites. Carbohydr Polym Oct 2005;62(1):19–24. https://doi.org/10.1016/j.carbpol.2005.07.015.
[44] Khazaei A, Nateghi L, Zand N, Oromiehie A, Garavand F. Evaluation of physical, mechanical and antibacterial properties of pinto bean starch-polyvinyl alcohol biodegradable films reinforced with cinnamon essential oil. Polymers 2021;13(16). https://doi.org/10.3390/polym13162778.
[45] Lani NS, Ngadi N, Johari A, Jusoh M. Isolation, characterization, and application of nanocellulose from oil palm empty fruit bunch fiber as nanocomposites. J Nanomater 2014;2014. https://doi.org/10.1155/2014/702538.
[46] S. Loganathan, R. B. Valapa, R. K. Mishra, G. Pugazhenthi, and S. Thomas, "Chapter 4 - thermogravimetric analysis for characterization of nanomaterials," in Micro and nano technologies, S. Thomas, R. Thomas, A. K. Zachariah, and R. K. B. T.-T. and R. M. T. for N. C. Mishra, Eds. Elsevier, 2017, pp. 67–108.
[47] Lomeli Ramirez MG, Satyanarayana KG, Manríquez-González R, Iwakiri S, Muniz G, Sydenstricker Flores-Sahagun T. Bio-composites of cassava starch-green coconut fiber: Part II-Structure and properties. Carbohydr Polym Feb 2014;102:576–83. https://doi.org/10.1016/j.carbpol.2013.11.020.
[48] Hafizulhaq F, Abral H, Kasim A, Arief S, Affi J. Moisture absorption and opacity of starch-based biocomposites reinforced with cellulose fiber from bengkoang. Fibers 2018;6(3). https://doi.org/10.3390/fib6030062.
[49] Tan SX, Andriyana A, Ong HC, Lim S, Pang YL, Ngoh GC. A comprehensive review on the emerging roles of nanofillers and plasticizers towards sustainable starch-based bioplastic fabrication. Polymers 2022;14(4). https://doi.org/10.3390/polym14040664.
[50] Gulati K, Lal S, Diwan PK, Arora S. Investigation of thermal, mechanical, morphological and optical properties of polyvinyl alcohol films reinforced with buddha coconut (Sterculia alata) leaf fiber. Int J Appl Eng Res 2019;14(1):170–9.
[51] Terzioglu Pinar, Par FN. Polyvinyl alcohol-corn starch-lemon peel biocomposite films as potential polyvinyl alcohol-corn starch-lemon peel biocomposite films as potential. Food Packaging 2020;16(December):373–8. https://doi.org/10.18466/cbayarfbe.761144.
[52] Wang G, Yang X, Wang W. Reinforcing linear low-density polyethylene with surfactant-treated microfibrillated cellulose. Polymers 2019;11(3). https://doi.org/10.3390/polym11030441.